https://doi.org/10.5194/hess-2020-34
Preprint. Discussion started: 26 February 2020

Hydrology and Earth System Sciences
Discussions

Drivers of nitrogen and phosphorus dynamics in a groundwater-fed urban catchment revealed by high frequency monitoring

Liang Yu[1, 2], Joachim C. Rozemeijer[3], Hans Peter Broers[4], Boris M. van Breukelen[5], Jack J. Middelburg[6], Maarten Ouboter[2], and Ype van der Velde[1]

[1]Faculty of Science, Vrije University Amsterdam, 1181HV, Amsterdam, the Netherlands
[2]Waternet Water Authority, 1096 AC, Amsterdam, the Netherlands
[3]Deltares, 3508 TC, Utrecht, the Netherlands
[4]TNO Geological Survey of the Netherlands, 3584 CB, Utrecht, the Netherlands
[5]Department of Water Management, Faculty of Civil Engineering and Geosciences, Delft University of Technology, Stevinweg 1, 2628 CN, Delft, the Netherlands
[6]Department of Earth Sciences, Faculty of Geosciences, Utrecht University, P.O. Box 80 021, 3508 TA, Utrecht, the Netherlands

Correspondence to: Liang Yu (xiaobaidrawing@gmail.com)

Abstract. Eutrophication of water bodies has been a problem causing severe degradation of water quality in cities. To gain mechanistic understanding of the temporal dynamics of nitrogen and phosphorus in a groundwater fed low-lying urban polder, we applied high frequency monitoring in Geuzenveld, a polder in the city of Amsterdam. The high frequency monitoring equipment was installed at the pumping station where water leaves the polder. From 2016 March to 2017 June, total phosphorus (TP), ammonium (NH_4), turbidity, electrical conductivity (EC), and water temperature were measured at intervals smaller than 20 minutes. This paper discusses the results at three time scales: annual scale, rain event scale, and single pumping event scale. Mixing of upwelling groundwater and runoff was the dominant hydrological process and governed the temporal pattern of the EC, while N and P fluxes from the polder were also significantly regulated by primary production and iron transformations. The mixing of groundwater and runoff water governed water quality through variation of the intensity and duration of the events. For NH_4, the dominant form of N in surface water originating from groundwater seepage, we observed low concentrations during the algae growing season, while concentrations were governed by mixing of groundwater and precipitation inputs in the late autumn and winter. The depletion of dissolved NH_4 in spring suggests uptake by primary producers, consistent with high chlorophyll-a, O_2, and suspended solids during this period. Total P and turbidity were high during winter, due to the release of reduced iron and P from anoxic sediment to the water column. Rapid Fe^{2+} oxidation in the water column is the major cause of turbidity. In the other seasons, P is retained in the sediment by iron oxides. Nitrogen is exported from the polder to the downstream water bodies throughout the whole year, mostly in the form of NH_4, but as organic N in spring. P leaves the polder mainly during winter, primarily associated with $Fe(OH)_3$ colloids and as dissolved P. Based on this new understanding of the dynamics of N and P in this low lying urban catchment, it is possible to formulate management strategies that can effectively control and reduce eutrophication situation in urban polders and receiving downstream waters.

Keywords: Nitrogen and phosphorus dynamic, high frequency monitoring, benthic algae, iron chemistry, Amsterdam, groundwater seepage

1 Introduction

Eutrophication is one of the most notorious phenomena of water quality impairment in cities, caused by excess inputs of N and P from wastewater treatment plants, storm runoff, overflow of sewage systems in cities with combined drainage systems, manure and fertilizer application in urban green areas and atmospheric deposition (Walsh et al., 2005; Kabenge et al., 2016; Toor et al., 2017; Yang & Toor, 2018; Putt et al., 2019). Recently, groundwater has been identified as another important source of N and P in cities situated in low-lying deltas (Yu et al, 2018 & 2019). The upwelling nutrients in groundwater, originating from the organic rich delta subsurface, end up in the surface water of cities and are transferred to downstream waters and

https://doi.org/10.5194/hess-2020-34
Preprint. Discussion started: 26 February 2020

Hydrology and Earth System Sciences
Discussions

eventually reach the coastal zones, where they may induce harmful algal blooms or cause hypoxia along coastlines (He and Xu, 2015; Beusen et al., 2016; Le Moal et al., 2019). Hence, it is of pivotal importance to understand N and P dynamics in the urban freshwater bodies in order to mitigate the input of nutrients into the oceans (e.g. Nyenje, et al., 2010; Toor et al., Paerl et al., 2016; 2017; Le Moal et al., 2019). Nutrients dynamics are governed by biological, chemical, and physical processes and their interactions.

Assimilation by primary producers is a major biological factor regulating N and P concentrations in aquatic environment. Aquatic micro- and macro-organisms assimilate P as PO_4 and N mainly in fixed forms such as nitrate (NO_3) and ammonium (NH_4), but for some specific organisms also in the form of N_2. NH_4 is the preferred N-form by microbes (Middelburg and Nieuwenhuize, 2000), but the uptake rate for both NH_4 and NO_3 can achieve maximum rates under sustained exposure of NH_4 or NO_3 (Bunch and Bernot, 2012). Moreover, the nitrogen species are also involved in redox transformations (Soetaert and Herman, 1995). Under anaerobic conditions, NO_3 can be reduced to NH_4, in particular with high organic matter contents, or denitrified to N_2 and N_2O (Mulder et al., 1995), the latter is a climate-active gas. Under aerobic conditions, NH_4 can be oxidized to NO_3 through nitrification by nitrifying microbes even under cold conditions (below 10 °C), which is an O_2 consuming, acid generating process (Painter, 1970; Wilczak et al., 1996; Cavaliere and Baulch, 2019).

The mixing of water from different flow routes is an important hydrological process that controls nutrient dynamics (Rozemeijer and Broers, 2007; Rozemeijer et al., 2010a; Van der Grift et al., 2014; Yu et al., 2019). As nutrient concentrations and speciation differ among different flow routes (Wriedt et al., 2007; Rozemeijer et al., 2010a; Yu et al., 2019; Yang and Toor, 2019), the mixing process results in the dilution or enrichment of nutrients in surface water bodies during events (Wang et al., 2016), and chemical reactions such as mineral precipitation with associated P incorporation cause removal from water column (Rozemeijer et al., 2010a; Van der Grift et al., 2014; Yu et al., 2019).

Retention is another factor that determines nutrient concentrations and transport (McGlathery et al., 2001; Zhu et al., 2004; Henry and Fisher, 2003), especially for phosphorus most of which is retained in inland water bodies sediment (Audet et al., 2019), either being permanently buried in the sediment or temporarily stored and acting later on as internal nutrient source (Kleeberg et al., 2007; Filippelli, 2008; Zhang et al., 2018). Multiple researchers have highlighted the influence of iron chemistry on the dynamics of P in pH neutral environment (Chen et al., 2018; Van der Grift et al., 2018). This is especially relevant when iron-rich groundwater interacts with surface water (Griffioen, 2006; Van der Grift, 2014), in which P is immobilized by the formation of iron(oxy)hydroxides during groundwater aeration. However, changes in chemistry or temperature may lead to the release of P and reduced iron. For instance, under anaerobic conditions, Fe and P can be mobilized by sulfate reduction, but this can be counteracted by the presence of NO_3 as the electron acceptor (Smolders et al., 2006).

Most studies of eutrophication are based on discrete sampling events which can give a general pattern of nutrient dynamics, but can easily miss important nutrient transport and processing phenomena (Rozemeijer et al., 2010; Rode et al., 2016; Toor et al., 2017). The countermeasures to control eutrophication have been hampered because of limited knowledge of N and P dynamics, for instance its response to changing weather conditions, land use, etc (van Geer et al., 2016). In recently years, high frequency technology has proved to be a way to understand nutrient dynamics (Rode et al., 2016; Van Geer et al., 2016; Bieroza et al., 2018). Due to the abundant information offered by this technology, combined methodologies have been developed to quantitively understand the in stream hydrochemistry of nutrients (Miller et al., 2016, Van der Grift et al., 2016, Duncan et al., 2017).

In our previous study on the water quality of Amsterdam (Yu et al, 2019), the transport routes of N and P from groundwater to surface water through seepage and drains were identified. In addition, spatial and temporal concentration patterns from discrete sampling campaigns showed a clear dilution pattern of other water quality parameters such as EC. However, the temporal patterns of N and P were still poorly understood, probably due to their reactive nature and more complex biogeochemistry. In order to obtain insight in the controlling mechanisms of N and P transport, we performed a year-round high-resolution N and P concentration monitoring campaign. The goal of this study is to understand the mechanisms that

https://doi.org/10.5194/hess-2020-34
Preprint. Discussion started: 26 February 2020

Hydrology and Earth System Sciences
Discussions

control the dynamics of N and P in urban delta catchments affected by groundwater, in order to contribute to the knowledge needed to formulate management strategies that can effectively reduce eutrophication of downstream waters. We conducted a one-year high frequency monitoring campaign in 2016-2017, measured parameters EC, NH_4, TP, turbidity and water temperature. The temporal patterns of these parameters were studied at three time scales: the annual scale, rain event scale, and pumping event scale, unraveling the hydrological and the reactive biogeochemical processes that control the nutrient dynamics at these 3 time scales.

2 Methods

2.1 Study site

Geuzenveld is a newly built urban polder on the west of the city of Amsterdam (Fig.1). Since 1990s, when it was converted from agricultural to urban land, it has developed into a highly paved area. Similar to other new neighbourhoods, Geuzenveld is equipped with a separated drainage system. A rain harvesting system was installed on all the buildings and houses in the polder, leading rain water from the roof and the street directly to the ditches, which results in fast and large amounts of runoff during storm events. Because Geuzenveld is a low-lying polder, a significant amount of groundwater seeps into the catchment constantly due to the constant water level in the primary channel and Geuzenveld. The groundwater head in the main aquifer and the shallow groundwater level in Geuzenveld are always much higher than the surface water level (Fig.2). To keep the foundations of the building dry, there is a groundwater drainage system placed under an artificial sandy layer, right on top of a natural clay layer. The drain elevations range from -4.84 to -4.61 m NAP (NAP: Normalized Amsterdam Peil, a known international standard conforming to mean sea level), which is below the groundwater level throughout the year, making sure that groundwater seepage always drains into the ditches.

The water system of Geuzenveld is connected to the secondary water channel to its east, then connected to the adjacent primary channel, called boezem, the Boezem Haarlemmerweg. The boezem water level is -2.10 m NAP. It is much higher than the target surface water level of Geuzenveld, -4.25 m NAP. The surface water level in polder Geuzenveld is controlled by a pump station, which is the main outlet of this polder, situated in the northeastern corner.

There are two pumps (Pump 1 and Pump 2) in the pumping station, and they have different start and end pumping threshold points (Table 1).

The two pumps are activated when the surface water level exceeds the triggering level which are furthermore separated as day and night triggering levels (Table 1). The capacity of each pump is 3.6 m^3 per minute. Most of the time, only one of the two pumps works and the surface water level is maintained between -4.31 m NAP and -4.23 m NAP, which are the night inactive and active pumping levels respectively. Normally, the surface water level drops immediately when the pump(s) start(s) working. Once the pump(s) stop(s), the surface water level will steadily rise due to the continuous inflow of groundwater seepage. During rainfall events, the surface water level will rise faster.

2.2 Monitoring network setup

2.2.1 High frequency monitoring

A high frequency monitoring network was built on a temporary floating platform in front of the pump station. The water flowed around and underneath this platform to the pumping station when the pumps started working. One year time series of NH_4-N (mg L^{-1}), TP (and ortho-P) (mg L^{-1}), turbidity (Formazin Nephelometric Unit, FNU), electrical conductivity (EC, µS/cm) and water temperature (°C) were collected by the following equipment: a Sigmatax sampler combined with a Phosphax sigma auto analyser for total phosphorus (TP), Amtax for NH_4-N combined with a Filtrax automatic sampler, a Solitax-tline sc for turbidity (manufactured by: Hach Lange GmbH Düsseldorf, Germany), and CTD-Diver for electrical conductivity (EC) and water temperature (manufactured by: Van Essen Instruments, Delft, The Netherlands).

https://doi.org/10.5194/hess-2020-34
Preprint. Discussion started: 26 February 2020

Hydrology and Earth System Sciences
Discussions

The Phosphax sigma is an analogue analyser for the high precision determination of total phosphorus concentration in accordance with EN 1189 Phosphormolybdenum Blue method. Samples are automatically taken through a Sigmatax sampling probe and include suspended solids. Subsequently, the sample is ultrasonic homogenized before delivery to the Phosphax sigma. It is digested by the sulphuric acid-persulphate method (APHAAWWA-WPCF, 1989), and analysed with a LED photometer (at 880 nm) (Hach, user manual of Phosphax sigma, 2016).

Samples for NH_4 are prepared by a filtration system, Filtrax. It continuously extracts samples through two ultra-filtration membranes (0.15 µm) plates. Particles get dispersed by a continuous aeration system near the surface of the membranes (The aeration caused severe build-up iron precipitants on the plates). The samples are then delivered to Amtax sc for analysis. The ammonium in the sample is first converted to gaseous ammonia. Only the NH_3 gas passes through the gas-permeable membrane of the electrode and is detected. This method guarantees a wide measuring range and is less sensitive to other compounds compared to methods that make use of an ion-selective electrode (ISE). The Amtax sc in our study was calibrating automatically at 22:00 every 24 hours before September 2016, every 48 hours thereafter. Maintenance work was conducted weekly as the tubes were easily blocked by iron precipitates (Hach, user manual of Amtax sc, 2013).

The Solitax-tline sc sensor is a turbidity sensor with dual-beam optics and added backscatter. The measuring principle is based on a combined infrared absorption scattered light technique that measures the lowest turbidity values in accordance with DIN EN 27027 just as precisely and continuously as high sludge contents. Using this method, the light scattered sideways by the turbidity particles is measured over an angle of 90° (Hach, User manual of Solitax sc, 2009).

The monitoring period of NH_4 and turbidity is from 2016-05-10 to 2017-06-16. Time series of phosphorus were obtained from 2016-05-23 to 2017-06-16. Electrical conductivity and temperature data are from 2016-06-10 to 2017-06-15. The NO_3 analyser, Nitratax, time series consistently showed an artificial drift and proved to be unreliable in our field setting, possibly due to biofilm accumulation in combination with iron oxides precipitation (see discussion). All the equipment outputs were integrated into one wireless station. The monitoring station was shut down several time by lightening, so an electricity restart program was also applied in this network. It worked for all equipment except for the Phosphax, which had to be restarted manually after a black out.

Precipitation (hourly) and Evapotranspiration (daily) data were downloaded from the Schiphol KNMI station which is about 2 km away from Geuzenveld. Hourly pumping activity and surface water level data were obtained from Waternet, the water authority in Amsterdam.

2.2.2 Low frequency monitoring

Since 2006, Waternet has monitored with a frequency of 12 times per year at the pumping station of Geuzenveld. Between 2016 and 2017, the sampling frequency became twice per month. Many parameters were measured in this dataset, but for this research we selected the following: (1) EC, NH_4 and TP to fill in the gaps in the continuous time series, and to verify and monitor the potential drift and offset of the high frequency data and (2) pH, O_2, HCO_3, suspended solids (detail of methods are described by Yu et al, 2019), chlorophyII-a, and transparency for further understanding the biogeochemical processes.

Bi-weekly total iron in the water column was analysed separately using ICP-AES (inductively coupled plasma-atomic emission spectrometry). Total Fe was analysed from samples to which $HgCl_2$ was added for preservation and that were stored in a dark and cool environment. To release all Fe that may have sorbed or precipitated during storage, we added 1 or 0.5 ml HCl in the water samples to dissolve eventual flocks, homogenized the samples in an ultrasonic bath for 24h, shook again to break down all the flocks, sampled 10 mL of the water with pipet into a Teflon bottle, added 3.2 mL HCl : HNO_3 3:1 for extraction, and subsequently put them in a stove at 90 °C for 24 hours. The final solutions were analyzed by ICP-AES. Blanks were included and treated identical to samples.

https://doi.org/10.5194/hess-2020-34
Preprint. Discussion started: 26 February 2020

Hydrology and Earth System Sciences
Discussions

2.3 Data processing and analysis

The time series data were analysed at 3 time scales: annual, rainfall events (several days) and single pumping events (several hours). At the annual scale, we introduced a linear mixing model to discern which part of the observed solute dynamics can be attributed to hydrological mixing and when additional chemical or biological processes are needed to explain the observed dynamics. The mixing model was based on the assumption that precipitation and groundwater seepage are the only water inlets, pumping and evapotranspiration are the only outlets, and pumping activity is the only way solutes leave the water system. In this model, we assumed a constant seepage rate. Accordingly, surface water level was calculated from:

$$\frac{dV}{dt} = \big(P(t) + S - E(t)\big) * A_{polder} - Pump(t) \quad (1)$$

$$L(t) = \mathrm{V(t)}/A_{ditch} \quad (2)$$

L is surface water level in the ditches, ***V*** is total water volume in the ditches, ***P*** is precipitation, ***S*** is a constant seepage, ***E*** is potential evapotranspiration, A_{polder} is area of the polder, A_{ditch} the area of the ditches in the polder. Water level ***L*** determines the activation of pumping activity. ***Pump(t)*** is water volume being pumped out with maximum capacity 216 $m^3\ h^{-1}$. Once ***L(t)*** exceeds the upper ranges of water level (start point, section 2.1), the pumps will start to pump until ***L*** goes below the stopping end (section 2.1) in the pumping scheme.

A complete mixing of solutes was assumed in the model, which means that seepage, ditch water and precipitation mix instantaneously when they enter the surface water. A delay from precipitation to run-off/drainage and to ditches was not specifically considered.

$$\frac{d(VC)}{dt} = S * A_{polder} * C_{gw} + P(t) * A_{polder} * C_P - Pump(t) * C(t) \quad (3)$$

C(t) is solute concentration at time t, C_{gw} is the average groundwater concentration, C_p is the average concentration in runoff, ***V*** is the ditch water volume given by equation (1).

Due to the high salt concentration of the seepage water, EC is a conservative water quality parameter (EC varies with Cl concentration in the ditch water, see supplement Figure S1 EC vs. Cl), which makes it a good index for linking groundwater and surface water in this system (see also Yu et al., 2019). In the model, seepage rate was adapted to get the best fit between the modeled and the measured EC. The final chosen seepage rate was 1.5 mm d^{-1}. Compared to EC, nutrients are highly reactive solutes sourced from groundwater and thus can vary a lot along their flow routes due to biogeochemical processes. The model above gave us a tool to simulate concentration dynamics under the assumption that EC, NH_4 and TP were conservative. By comparing the modeled EC, NH_4-N and TP with high frequency measurements, potential processes that might deprive or enrich nutrients along the flow routes were inferred from the discrepancies between the modeled and the measured data. The simulated concentrations of EC, NH_4-N and TP were plotted together with their high frequency measured time series. The average concentration of EC in groundwater was set equal to the average of the sampling survey, which was 1750 µS/cm (including both deep and shallow groundwater, Yu et al., 2019). For the NH_4 and TP concentration data, we chose the measurement from a drain sampling point (Drain 3, Yu et al., 2019) in the middle of the polder as the non-disturbed groundwater collected by the drains in this area of the polder. They were 8.1 mg N L^{-1} and 1.6 mg L^{-1} respectively. The starting (01-01-2016) concentrations were 1200 µS/cm, 4 mg L^{-1}, and 2 mg L^{-1} for EC, NH_4, and TP respectively. The results were not very sensitive to selected end-member values.

The time series data were further analysed at shorter scales: rain event scale and pumping event scale. Four rain events were selected according to the dilution extent of EC, they were: 10-06-2016 ~ 15-07-2016, 15-08-2016 ~ 26-09-2016, 10-11-2016 ~ 05-01-2017, and 20-02-2017 ~ 10-04-2017. These four events covered both EC dilution during rainfall and the recovery afterwards in different seasons. We selected 4 representative pumping events to present the response of EC, NH_4, TP, and turbidity to the pumping activities. Those events were in 15-07-2016 ~ 17-07-2016, 27-10-2016 ~ 29-10-2016, 20-12-2016 ~ 22-12-2016, and 05-05-2017 ~ 07-05-2017.

https://doi.org/10.5194/hess-2020-34
Preprint. Discussion started: 26 February 2020

Hydrology and Earth System Sciences
Discussions

3. Results

The hydrological time series of groundwater and surface water levels and pumping activity, and meteorological time series of rain and evapotranspiration provided the basis for understanding the behavior of the water quality parameters (EC, NH_4, TP, turbidity, Fe and O_2). Their annual patterns will firstly be discussed and then be explored by comparing the observations with the predictions based on conservative, full mixing behavior. Next, the water quality parameters will be studied at two smaller time scales: i.e. the event and pumping-event scales to derive information about the shorter time scale dynamics and controlling processes.

3.1 Annual pattern of meteorological, hydrological, and water quality time series

3.1.1 Meteorological and hydrological conditions in polder Geuzenveld

To explain the time series (Fig. 2), we distinguish between dry/wet periods and dry/wet seasons. The wet and dry periods (days to weeks) are represented by a water surplus (blue color in Fig.2B, daily evapotranspiration < daily precipitation) or a water deficiency (pink color in Fig.2B, daily evapotranspiration > daily precipitation). The wet season was from October 2016 until the end of February in 2017; consequently, the rest is considered as the dry season. The wet season is distinguished by a higher frequency of pumping and lower water temperatures (Fig.2B). Water temperature ranged from 2 to 26 ℃. From June to mid September 2016, the temperature remained above 18 ℃, then declined to become lower than 10 ℃ at the end of October. The following four months (November to February) were the coldest. Especially in January and February 2017, there was a considerable period that the water temperature was below 3 ℃. By the end of February temperatures started to rise again to reach 10 ℃ by the end of March 2017.

The surface water level in Geuzenveld has been maintained between -4.31 and -4.1 m NAP, strictly regulated by pumping (Fig.2A). After the pumps stopped, the surface water level recovered faster during the wet season (between October 2016 and March 2017) than during the dry season. Similarly, the shallow groundwater level positively corresponded to the precipitation and negatively to the daily accumulative pumping volume. The shallow groundwater level in Fig.2A was from one of the piezometers, which lies right outside of the polder. In contrast to the constant water level ranges from surface water regulation regime, the shallow groundwater had relatively low levels in the wet season compared to the dry season. This might have been caused by the water level regulation of the boezem Haarlemsmeer with higher levels in summer than in winter. Groundwater levels were consistently 20-40 cm higher than the surface water level in the polder, which confirms the continuous groundwater seepage into the surface water system.

3.1.2 Annual water quality patterns

During a rainfall event, rain and runoff from pavements and roofs, which are collected by a separate drainage system, directly feed the surface water (Fig.1). Distinct rainfall events cause a strong dilution pattern of both EC and NH_4 (in Fig.2C). The EC ranged from 600 to 1500 µS/cm. In general, during rainfall events, the EC declined because of dilution, while, after the events, EC gradually rose back up to around 1500 µS/cm if there was no rain. This duration of the return to pre-event EC values, i.e. *recovery time*, was longer in the wet season than in the dry season. A similar pattern of dilution and recovery is also visible for NH_4, especially for the period August 2016 – March 2017. However, a contrasting pattern without NH_4 recovery occurred twice: from the middle of June to the end of August 2016 and from the middle of March to the middle of May 2017. During these periods, concentrations of NH_4 were considerably lower and deviated from the slope of the EC pattern. During the first period NH_4 decreased from around 4 mg L^{-1} to around 2 mg L^{-1} and during the second period reached down to almost 0 mg L^{-1}. Note that during these periods the pattern of NH_4 deviated from EC, whereas during the rest of the time NH_4 followed the dilution and recovery pattern of EC, especially between the end of November and the beginning of March. At the beginning

https://doi.org/10.5194/hess-2020-34
Preprint. Discussion started: 26 February 2020


Hydrology and Earth System Sciences
Discussions

of May 2016, before the setup of the high frequency monitoring network, a discrete water sample confirmed the low NH_4 concentration during this time of year.

Both TP and turbidity showed contrasting patterns during the wet and dry seasons (Fig. 2D). Turbidity was constantly below 100 FNU, mostly below 50 FNU until October when it suddenly substantially raised up to 500 FNU (more details refer to Figure S2 in supplementary information). A drop to about 200 FNU occurred right after this first peak, which seemed to correspond to excessive precipitation (Fig.2B). Soon turbidity went up again and peaked at 1800 FNU. Turbidity stayed around 200 FNU from the middle of November 2016 until April 2017. Since then, turbidity levels had stayed around 200 FNU until the middle of April 2017. It was lower than 50 FNU since then.

Before the middle of November 2016 and after March 2017, TP fluctuated around 0.5 mg L^{-1}, but always below 1 mg L^{-1}. TP concentrations significantly increased starting from the middle of November. During the wet season with the low temperatures, TP almost constantly stayed above 1 mg L^{-1} and even reached values of about 3 mg L^{-1} in December. Although there were large gaps in the TP time series during this period, the high TP concentrations appear to have been diluted by rain events, for example the event at around January 10th, 2017. Most discrete samples measurements of TP matched well with values from the time series (Fig.2D).

Total-Fe concentrations were most of time lower than 2 mg L^{-1} (Fig. 2E), but for the wet season when concentrations were higher and reached up to about 6 mg L^{-1}. The initiation of Fe increases at the beginning of the wet season coincided with that of turbidity (Fig.2D). Upon the increasing temperature in March 2017, total Fe concentrations dropped back to below 2 mg L^{-1}. Dissolved O_2 concentrations were generally low in the water column; i.e. usually below 5 mg L^{-1}. Concentrations of over 3 mg L^{-1} were only found in March, April and May.

3.2 Model of water quality time series based on water balance

A simple fixed-end-member mixing model was used to predict the conservative mixing of EC, NH_4, and TP. The simulated and the measured EC, NH_4, and TP are plotted in Figure 3. Figure 3(A) shows that predicted and observed EC agree reasonably, especially from May to November 2016. After that, the conservative mixing approach underestimated EC but the main patterns were still reproduced. Accordingly, the observed dynamics of EC are consistent with mixing of high EC seepage water with low EC runoff water.

Predicted and observed NH_4 concentration generally agree, in particular the recovery after a dilution event is captured well. However, during the dry summer of 2016 and spring of 2017, predictions based on conservative mixing are higher than observations. Concentrations of TP are usually below expectations based on conservative mixing, except during the period from the end of November to the beginning of March. During this period, TP showed distinct peaks up to 3 mg L^{-1}, but a similar base-level concentration as expected from the mixing model.

3.3 Water quality responses to single events analysis

To elucidate the response pattern of water quality to precipitation and pumping activity, we selected four major events (Fig.1 (red blocks) and Figure 4) and four pumping events (Figure 5). The former events were chosen according to their significant dilution pattern of EC (Fig.4), while the latter were pumping events without occurrence of rainfall (Fig.5). All seasons were covered, including some of the wet and dry periods.

3.3.1 Rainfall events

EC and NH_4 showed clear dilution and recovery patterns during all events, while the pattern was not clear for TP and turbidity (Fig.4). The extent of dilution of EC appears to depend on the precipitation intensity. Rainfall during the recovery period determined how long it took to recover back to the highest level. The short but intensive rainfall during events 1 and 2 reduced EC rapidly from around 1300 to around 700 µS/cm, while the recovery took about 1 month. Events 3 and 4 had less rainfall

https://doi.org/10.5194/hess-2020-34
Preprint. Discussion started: 26 February 2020


Hydrology and Earth System Sciences
Discussions

and dilution of EC was less (from about 1300 to about 800 µS/cm) and recovery took more than one and a half month in event 3, during which multiple small events occurred. The dilution patterns in the NH_4 continuous time series for events 1 and 2 were similar to those of EC, while no such patterns were present for events 3 and 4, partly due to data gaps. Moreover, the dilution effect on NH_4 is much less significant than the drops in spring and summer, as stated before.

The response of TP to these events varied. Following event 1, TP concentrations were diluted from about 0.75 to about 0.4 mg L^{-1}, subsequently TP recovered to 0.8 mg L^{-1} in a short time. The response during period 2 is unclear because of too many data gaps. In events 3 and 4, TP concentrations were low due to the less intensive but longer periods of rainfall. However, following event 3, TP concentrations increased to 3 mg L^{-1} when rain was absent during the recovery period. No such pattern was found during event 4.

During the dry season (with event 1 and 2 included) turbidity always stayed below 50 FNU. Turbidity sometimes showed single peaks which are likely related to disturbances of the floating platform by wind and should probably be treated as false signals. Turbidity had much higher pre-event levels for events 3 and 4. During event 3, turbidity was reduced by about 300 FNU and then recovered. After recovery branch, some peaks of turbidity were observed that co-occurred with those of TP. In event 4, turbidity was also reduced by about 100 FNU by the first rain event at the beginning, corresponding with the dilution of EC at the same time. There were some turbidity spikes after the recovery after event 4.

3.3.2 Pumping events and day and night pattern

In artificial lowland catchments, water systems are intensively regulated by pumping activity to prevent flood and drought. However, there is a substantial lack of knowledge about the possible consequences of such regulation on aquatic ecology and water quality. Significant peaks in P by the activation of pumps was observed by Van der Grift in his high frequency monitoring campaign in an agriculture lowland polder (Van der Grift et al., 2016). In this study, we conducted a monitoring in a much smaller catchment and in a more shallow and narrow urban water course, partly in order to find out how nutrient concentrations respond to the pumping activity. The selected pumping events covered four seasons: summer (2016 July, event 1), autumn (2016 October, late autumn, event 2), winter (2016 December, event 3) and spring (2017 May, event 4) (Fig.5).

The diurnal variation of EC is rather small compared to the variations observed at the rain event scale; EC varies less than 150 µS/cm (Fig. 5). While EC and NH_4 often co-varied on the rain event time scale, they showed opposite behavior in 3 out of 4 pump-events. Pumping has the least influence on NH_4 in winter. Similarly, during events 2, 3 and 4, TP and EC are positively correlated, while no clear pattern was observed during summer (pump event 1). TP decreased during the pumping activity in summer (around 0.04 mg L^{-1}) and autumn (around 0.1 mg L^{-1}), but the changes are much smaller than in winter (decreased around 0.7 mg L^{-1}) and spring (increased around 0.3 mg L^{-1}). Turbidity was elevated during pumping events 1 and 3, but reduced by pumping in the late autumn and spring. A small, abrupt rise of turbidity occurred during pump event 1 (summer) from 10 to 50 FNU. Turbidity was also elevated (> 300 FNU) during pump event 3 (winter). Event 2 caused a major drop in turbidity (more than 1000 FNU). The response of turbidity to the pumping events appears to be influenced by the pre-event conditions.

4. Discussion

This study aimed at understanding the dynamics of N and P fluxes from the low-lying urban polder of Geuzenveld to downstream surface waters in order to support water managers to mitigate eutrophication. Based on our high-resolution water quality measurements, we found that the surface-water chemistry at the polder outlet pumping station is governed by a complex combination of hydrological mixing and biogeochemical processing. In the following discussion, we start with the relatively straightforward dilution behavior of EC, followed by adding the impact of primary production (i.e. algae growth) for

https://doi.org/10.5194/hess-2020-34
Preprint. Discussion started: 26 February 2020


Hydrology and Earth System Sciences
Discussions

understanding the NH_4 concentration patterns, and benthic primary producer and iron chemistry for understanding the turbidity and TP concentration patterns.

4.1 Hydrological mixing between groundwater and rainfall

In a highly manipulated low-lying urban catchment like Geuzenveld, mixing between rainwater and groundwater in the ditches is fast due to the high fraction of impervious area and the installation of both a rainwater and a groundwater drainage system that transport these contrasting water types efficiently to the ditches (Yu et al., 2019; Walsh et al., 2005). Runoff in Geuzenveld has waters with an EC of about 166 µS/cm (Yu et al., 2019), which is low compared to the groundwater (1746 µS/cm on average). As a relatively conservative water quality parameter, mixing between rainwater and groundwater should be the main process for EC. This presumption is supported by the mixing model result of EC, which revealed close similarity to the measurements (Fig.2). Precipitation diluted EC values (Fig.2D and Fig.4). Moreover, the extent of dilution depended on the intensity of precipitation; heavy rainfall resulted in low EC values. In the absence of rainfall, EC values were sustained around 1500 µS/cm by the constant contribution of the groundwater. Changes in EC during pumping events were rather limited (Fig.5), possible reasons might be related to the pre-event conditions, or because the incomplete mixing of waters towards the pumping station. Therefore, the mixing between groundwater and rainwater may be more complicated during the pumping events.

Apart from the mixing between groundwater seepage and rainwater, road salts in urban runoff may also have an effect on EC values during the winter. Across the polder there are busy streets and road salts might be used extensively during cold winter days. During the monitoring campaign, freezing condition occurred from November onwards, when the modeled EC started to drift underneath the measurement (Fig.2). Road salts could therefore be a reason for elevated EC measurements during this period. However, neither the chloride nor the EC discrete sampling data showed the sign of road salt (Data not shown, refer to Figure S1 in supplementary information). This might be because that the discrete sampling was not able to catch the peaks of EC and Cl as residence time of water in the system is shorter in winter due to frequent pumping. Another possible reason for this drift might be the variation of groundwater discharge during different seasons. As we illustrated before in Fig. 2, the water level recovered faster in winter than other seasons indicating the increase of groundwater influx, which may be related to more saturated soils and faster delivery of water through the groundwater drain system.

During winter, mixing can also explain the NH_4 and TP patterns (Fig.3). Compared with groundwater, which carries around 8 mg L^{-1} NH_4 and 1.6 mg L^{-1} TP, rain and runoff have much lower nutrient concentrations, which makes groundwater the main nutrients source (Yu et al., 2019). It mixes with rainwater in the ditches through direct seepage and the efficient groundwater drainage systems. However, the mixing assumption cannot explain the behavior of NH_4 and TP during other seasons, when NH_4 and TP measured time series drift far below from the conservative mixing model pattern because of biological and chemical processes.

4.2 Primary production and nutrients

While NH_4 dynamics during winter can be explained by mixing, this is not the case during spring and summer because biological processes are then overruling physical mixing. This resulted in much lower measured NH_4 concentrations than calculated by our conservative mixing model during the growing season, benthic and planktonic primary producers (e.g. phytoplankton) assimilate nutrients and are an important factor controlling nutrient dynamics in rivers, lakes, streams (Hansson, 1988; Jäger et al., 2017). In polder Geuzenveld, the biological nutrient uptake is not only reflected in the time series data (Fig.2 and 3) but is also evident in the monthly measurements from the water authority for the period 2007-2018, summarized in Figure 6.

The increasing availability of light (and temperature increase) during spring, induces growth of primary producers. Growth of primary producers results in a consumption of ammonium, phosphate and silicate and a production of suspended solids, chlorophyll and oxygen, and a relatively higher pH (uptake of CO_2) (Fig.6). Primary production occurs both in the water

https://doi.org/10.5194/hess-2020-34
Preprint. Discussion started: 26 February 2020


Hydrology and Earth System Sciences
Discussions

column by phytoplankton as well as by benthic algae. Macrophytes could in principle also contribute, but they were absent in Geuzenveld. One of the structuring factors governing the relative importance of benthic and planktonic primary producers is light availability: benthic algae and macrophytes tend to dominate in shallow and clear waters, while phytoplankton is more likely to dominate in deeper and more turbid waters (Hartwig, 1978; Jäger and Borchardt, 2018; Petranich et al., 2018; Middelburg, 2019). Although our data do not allow conclusive determination whether benthic or pelagic primary producers dominate, it appears that their relative importance varies with season.

These primary producers also compete for nutrients. Benthic primary producers have direct (macrophytes) or first (benthic algae) access to nutrients that seep up from the subsurface, while planktonic primary producers depend on nutrient supply from surface runoff and nutrients remaining after consumption by benthic primary producers. For example, Henry and Fisher (2003) found that benthic algae can remove up to 80% of nitrogen from an upwelling water source. As we stated above, nutrient-rich groundwater is the major source of N and P to surface waters in polder Geuzenveld. In addition, due to the shallow depth of the ditches, light reaches the bottom with the consequence that benthic algae can proliferate in this polder. These benthic primary producers might utilize the up-flowing nutrients from groundwater and significantly intercept the nutrients from seeping further into the water column (Hansson, 1988; Pasternak et al., 2009). The increasing light availability and thus primary production during spring led to the nearly complete deprivation of NH_4 in the water column (Fig.2C).

Following the spring bloom, concentrations of chlorophyII-a (proxy for phytoplankton biomass) and O_2 dropped substantially, while NH_4 concentrations rapidly recovered to around 4 mg L^{-1} in both the time series (Fig.2C) and the long term monthly sampling results (Fig.6). Dissolved O_2 remained low (close to hypoxia) during the whole summer (below 2 mg L^{-1}) (Fig.2E and Fig.6), indicating that oxygen consumption by organic matter degradation and re-oxidation of reduced components from groundwater seepage outcompeted oxygen production from primary production. During summer, suspended solid and chlorophyll-a concentrations were low (Fig.6), indicating low biomass of plankton algae. Suspended solid and phytoplankton dominate light attenuation (Scheffer, 1998; Middelburg, 2019). Consequently, during this period, we observed an abrupt shift of the water regime from a turbid state to completely clear, as reflected in the high transparency from June to September (Fig. 6). The low biomass of phytoplankton might be due to N limitation as nutrients are intercepted by benthic algae at the sediment interface. An alternative explanation is that zooplankton grazing maintained phytoplankton biomass low (Strayer et al., 2008; Genkai-Kato et al., 2012).

Temperature and light reaching the sediment started to fall from September onwards, thereby reducing the intensity of biological activity, including NH_4 assimilation. Consequently, NH_4 started to behave conservatively again like EC (Fig.2 & Fig.3). The best fit between the modeled and measured NH_4 was from the end of November to the beginning of March, i.e during the winter period with lower light levels and shorter day lengths and very low primary production. The absence of primary production during winter, leads to conservative behavior of NH_4 governed by the mixing between groundwater and rain water.

Apart from primary production, NH_4 can also be consumed by nitrification, i.e. oxidation of NH_4 to NO_3 by microbes (Zhou et al., 2015). The produced NO_3 can be taken up by primary producers and by microbes reducing it to dinitrogen gas (denitrification and anammox ($NO_3 + NH_4 \rightarrow N_2 + H_2O$); Thamdrup and Dalsgaard, 2002; Kuenen, 2008). These NO_3 consuming processes were very active as NO_3 concentration were sometimes high (e.g.50 mg L^{-1}) in street runoff samples (Yu et al., 2019), but low in surface waters (Fig. 6).

4.3 P binding and turbidity

Iron chemistry is considered the dominant process governing the P dynamics in shallow groundwater fed ditches (Lijklema, 1994; Smolders et al., 2006; van der Grift et al., 2018). However, primary producers take up P for growth and at the same time release O_2 that regulates iron chemistry in lake water column (Spear et al., 2007; Zhang and Mei, 2015; Lu et al., 2016). This web of interactions likely controls P dynamics in these ditches.

https://doi.org/10.5194/hess-2020-34
Preprint. Discussion started: 26 February 2020


Hydrology and Earth System Sciences
Discussions

From spring to autumn, TP concentrations were fluctuating around 0.5 mg L^{-1}, and the water had low turbidity, thus high transparency allowing the growth of benthic algae that produce oxygen. Consequently, when P and Fe rich anoxic groundwater reaches the surface water-sediment interface, Fe oxidized into iron hydroxides in a short time (Van der Grift et al., 2014). P is then sorbed onto those Fe-hydroxides and retained in sediments. Oxidation of reduced iron consumes O_2, contributing to the low O_2 conditions of the water column (Fig.2E). Moreover, it leads to the formation of a reddish-brown film of ferric iron (hydrous ferric oxide, Baken et al., 2013; van der Grift et al., 2018) on the bottom of the ditches, which can be seen in summer when the water was transparent. This slimy layer comprising iron hydroxides and benthic microbes can easily be resuspended and therefore act as a source of turbidity following perturbations by pumping, wind, rain or foraging fish, e.g. event 1 (Fig.5). Lu et al (2016) showed that co-precipitation of P with metal oxides was stimulated by periphytic biofilm activity that increased the water pH. Consistently, a relatively higher pH was also observed in our spring monthly samples (Fig.6).

From the late autumn onwards, turbidity and total Fe concentrations significantly increased (Fig.2), the water turned brownish and transparency declined (Fig.6). Iron-rich particles are the most likely source of turbidity in freshwater (Lyvén et al., 2003; Gunnars et al., 2002; and Lofts et al, 2008). The suspension of these brownish iron colloids was likely stabilised by the presence of the dissolved organic matter (Mosley et al., 2003; Van der Grift et al., 2014), which (DOC) increased up to 18~33 mg L^{-1} during events (Supplementary information Figure S3). In the late autumn, the anoxic/oxic interface shifts from the sediment into the water column and so does the locus of colloid formation. The ditch sediment, which had benthic algae activity releasing O_2 during spring and summer, became anoxic in the fall by the upwelling of the anoxic groundwater. The anoxic seepage occurs year-round, but the production of oxygen by the benthic algae creates an anoxic-oxic transition at the water-sediment interface, which leads to iron hydroxides precipitation in the slimy layer at the bottom that disappears after the algae die off. As a consequence, Fe oxidation moved into water column where the conditions were relatively oxic (Van der Grift et al., 2014). Nevertheless, there was probably still enough Fe or other mineral oxides, such as aluminum hydroxide (Kopáček et al., 2005), binding capacity in the sediment for the fixation of P, as P concentrations remained low during this first turbidity peak.

During winter, temperatures were below 5°C, pH values were relatively lowered, and TP achieved its peak concentrations (Fig.2D). During this period, iron reduction in the sediments continued, P bounded to iron oxides gradually got released along with reduced iron (Li et al., 2016). In the water column, reduced iron was oxidized but much slower than during spring-autumn due to the lower temperatures (Van der Grift et al., 2014), and dissolved P was incorporated with the result that particulate P concentrations and turbidity became high (Yu et al., 2019).

4.4 Process synthesis

With the presence of benthic algae, abundant organic matter and bacteria, the sediment functions as an active environment for biotic processes (such as primary production and nitrification-denitrification-anammox) and abiotic processes (such as iron oxidation). Figure 7 shows a conceptual diagram for the N and P dynamics in this lowland urban catchment during the four seasons.

Spring: The improved light (and temperature) conditions stimulated primary production and nutrient uptake (N, P, Si) by phytoplankton and benthic algae. The resulting oxygen production caused oxidation of reduced iron from groundwater and the formation of iron oxides at the sediment surface. P was mostly bounded to this particulate iron instead of being released into the upper water layer. In this period turbidity was relatively low, but suspended solids reached a high concentration due to the phytoplankton.

Summer: N and P were still being uptaken by biological processing, in particular benthic algae. Phytoplankton biomass decreased because of competition for N or grazing activity. Benthic algae produced O_2, which in turn was used to oxidize all reduced iron reaching the sediment-water interface and P was still retained by iron hydroxides in the sediment. The water column was transparent (low TP and phytoplankton biomass) and relatively low in oxygen (because of warming).

https://doi.org/10.5194/hess-2020-34
Preprint. Discussion started: 26 February 2020

Hydrology and Earth System Sciences
Discussions

Late autumn: Biological activity declined (colder and less light), and more NH_4 reached the water column. Moreover, the redox zone moved from the sediment-water interface into the water column; the oxidation of Fe in the water column caused a peak of turbidity. P was still bounded by mineral compounds in the sediment.

Winter: During winter, NH_4 and TP showed the highest concentrations because of low biological activity. Iron oxides in the sediment dissolved under reductive and organic matter abundant conditions and released Fe^{2+} and P into the water column. NH_4 and EC dynamics were primarily governed by the conservative mixing between groundwater and precipitation/runoff.

4.5 Event scale N and P dynamics

At the event scales, N, P and turbidity were all reduced by dilution from precipitation/runoff. For P and turbidity, this effect was especially evident in the late autumn and winter. The responses to precipitation and pumping events were very different from those reported in the literature. Rozemeijer et al. (2010b) studied an agricultural catchment and found that rainfall events led to NO_3 decreases and P increases. Miller et al. (2016) observed NO_3 decreases during large discharges in an urban catchment. The lowering of turbidity in response to events in our urban catchment differs from observations in literature (van der Grift et al., 2014, Rozemeijer et al., 2010b). In agriculture areas, turbidity usually peaks in response to rainfall events due to erosion and remobilization of sediments. In an urban, paved environment erosion may be limited and runoff water has a low turbidity. Moreover, in the case of turbid pre-event conditions, fresh precipitation water flushes away this turbid water. In addition, Yu et al. (2019) showed that precipitation runoff delivers particles and O_2 to the ditches; this accelerates the further aggregation of the iron complexes. The resulting larger particles more readily settle to the bottom, causing a reduction of turbidity during events (Fig. 4).

Van der Grift et al. (2014) studied agricultural areas and observed that P and turbidity were significantly increased by pumping events. However, in our study, the effects of pumping activity on N, P and turbidity dynamics were variable, depending on the season. During the phytoplankton bloom in spring, activation of pumps resulted in flushing and as a result reduced turbidity during the event (Fig. 5 event 4). Consequently, phytoplankton was transferred to the downstream channel and added to the total N pool in that system. In summer (Fig.5 event 1), the dead detritus and the layer of iron compounds at the sediment surface were easily resuspended and contributed to turbidity peaks at the beginning of the pumping, but the materials also re-sedimented almost immediately once the flow reached stability. Resuspension also resulted in a significant increase of NH_4 in the water column which then was being pumped out (Fig.5 event 1). During late autumn, the water was highly turbid because of the formation of iron hydroxide colloids in the water column. The activation of the pumps caused export of these colloids and particles and thus reduced turbidity (Fig.5 event 2). The decline continued even after the event stopped because of particles settling and O_2 availability which stimulated the aggregation and sedimentation of the colloids. Moreover, NH_4 increased again by the pumping activity and was transferred downstream (Fig.5 event 2). The eventual impact of regulation of the Geuzenveld water system turns the pumping discharge into a point source for nutrients to downstream water bodies as shown in Figure 8.

Fluxes of N and P were highest during winter (Fig 6). These high fluxes are caused not only by the more frequent pumping activity, but also by the higher concentration of N and P in the water column in winter. In the time series data, NH_4 (the major form of N), had concentrations above 2.4 mg N L^{-1}(the local environmental quality standard (EQS) for N-total) , in all seasons except spring. NH4 concentrations even reached up to 6.5 mg L^{-1}. TP concentrations were constantly higher than 0.15 mg P L^{-1} (the local EQS); during winter it was always over 1 mg P L^{-1}. Although the NH_4 flux in the discharge was very low in spring (Fig.8), the actual total N flux might be much higher, as organic N (phytoplankton) was the major form of TN instead of NH_4 during this period (Fig.6 NH_4/N). Therefore, even though water authority measures have been effective in controlling the water quantities in the polder, it had unanticipated impact on nutrients export to the downstream water bodies. In order to prevent eutrophication in the urban waters, nutrient rich discharge from these areas are exported directly to the North-Sea Canal and to the North Sea.

https://doi.org/10.5194/hess-2020-34
Preprint. Discussion started: 26 February 2020

Hydrology and Earth System Sciences
Discussions

5. Conclusions

This study aimed at improving our understanding of the mechanisms that control the temporal patterns of nutrients and other water quality parameters in an urban catchment at three different time scales: annual scale, rain event and pumping event scale. Time series of EC, NH_4, TP, and turbidity were obtained by applying a high frequency monitoring technology for one year (May 2016 to July 2016). Observed EC, NH_4 and TP could only partly be explained by conservative mixing of groundwater and precipitation components. In particular, N and P fluxes in the shallow ditches were also impacted by biogeochemical processes, such as primary production and iron redox transformations.

(1) NH_4, the dominant form of N in surface water, originates primarily from groundwater seepage, and concentrations are lowered by primary producers (phytoplankton and benthic algae) in the growing season. High algal biomass was also clear from high chlorophyII-a and suspended solids in the water column.

(2) TP showed high concentrations in winter, but low concentrations in other seasons. Iron redox chemistry was the dominant process controlling the P dynamics in shallow groundwater fed ditches. P dynamics may also have been partly influenced by primary production which consumes P for growth and at the same time produces O_2 influencing the redox status in the sediments and in the water column.

(3) High turbidity levels occurred in the late autumn and winter, mostly in the form of iron hydroxides. It is resulted from a shift of the anoxic/oxic interface where the formation of iron hydroxides moves from the sediment towards the water column.

(4) Water pumped from the polder to downstream water bodies was rich in NH_4 from summer to winter, but rich in organic N in the form of algae during spring. P leaves the polder mainly during the winter season when it is released from the sediment and exported mostly in the form of P sorbed to $Fe(OH)_3$ colloids and as dissolved P.

(5) Precipitation diluted concentrations of most water quality parameters, but delivered O_2 to the water column, and in that way indirectly affected P and turbidity by intensifying iron oxidation and precipitation.

Our understanding of the N and P dynamics in this low-lying urban catchment may contribute to the development of effective water management strategies that reduce eutrophication conditions in both the urban polders and the downstream waters. Drainage of very low-lying areas (for use as residential and/or agricultural areas) not only increases pumping costs, but can also result in difficult to manage water quality conditions. Controlling the source, redirecting and utilizing the drainage water might be a strategy to reduce the input of N and P from groundwater into surface water. In addition, we showed that in lowland urban areas with high seepage rates the reactivity of the streambed sediments largely controls water quality of surface waters and thus should be managed with care when cleaning the surface water systems.

Acknowledgements

This work was funded through China scholarship council (no. 201309110088) and supported by Waternet, the Strategic Research Funding of TNO and Deltares. We highly appreciate the help and support from our Waternet co-workers: Eelco Wiebenga, Henk Molenaar, Sonja Viester, Laura Moria, and Frank Smits.

References

Audet J., Zak D., Bidstrup J., and Hoffmann C.C.. Nitrogen and phosphorus retention in Danish restored wetlands. Royal Swedish Academy of Sciences, 1-13, 2019. https://doi.org/10.1007/s13280-019-01181-2

Bunch N.D. and Bermot M.J.. Nitrate and ammonium uptake by natural stream sediment microbial communities in response to nutrient enrichment. Research in Microbiology. 163(2): 137-141, 2012.

Beusen A.H.W., Bouwman A.F., van Beek L.P.H., Mogollón J.M., and Middelburg J.J.. Global riverine N and P transport to ocean increased during the 20th century despite increased retention along the aquatic continuum. Biogeosciences. 13: 2441-2451, 2016.

Bieroza M.Z., Heathwaite A.L., Bechmann M., Kyllmar K., and Jordan P.. The concentration-discharge slope as a tool for water quality management. Science of the Total Environment, 630: 738-749, 2018.

Baken S., Sjostedt C., Gustafsson J.P., Seuntjens P., Desmet N.. Characterisation of hydrous ferric oxides derived from iron-rich groundwaters and their contribution to use suspended sediment of streams. Applied Geochemistry, 39: 59-68, 2013.

Cavaliere E. and Baulch H.M.. Winter nitrification in ice-covered lakes. PLoS ONE, 14(11): e0224864, 2019. https://doi.org/10.1371/journal.pone.0224864

Chen M., Ding S., Chen X., Sun Q., Fan X., Lin J., Ren M., Yang L., and Zhang C.. Mechanisms driving phosphorus release during algal blooms based on hourly changes in iron and phosphorus concentrations in sediments. Water Research, 133: 153-164, 2018.

Duncan J.M., Welty C., Kemper J.T., Groffman P.M., and Band L.E.. Dynamics of nitrate concentation-discharge patterns in an urban watershed. Water Resources Research, 53: 7349-7365, 2017. doi: 10.1002/2017WR020500

Filippelli M.G.. The global phosphorus cycle: Past, present, and future. Elements, 4(2): 89-95.

Griffioen J.. Extent of immobilisation of phosphate during aeration of nutrient-rich, anoxic groundwater. Journal of Hydrology, 320 (3-4): 359-369, 2006.

Gunnars A., Blomqvist S., Johansson P., and Andersson C.. Formation of Fe (III) oxyhydroxide colloids in freshwater and brackish seawater, with incorporation of phosphate and calcium. Geochim. Cosmochim. Acta, 66 :745-758, 2002.

Genkai-Kato M., Vadeboncoeur, Liboriussen L., and Jeppesen E.. Benthic-planktonic coupling, regime shifts, and whole-lake primary production in shallow lakes. Ecology, 93(3): 619-631, 2012.

Hansson L.A.. Effects of competitive interactions on the biomass development of planktonic and periphytic algae in lakes. Limnology and Oceanography, 33(1): 121-128, 1988.

Hartwig E.O.. Factors affecting respiration and photosynthesis by the benthic community of a subtidal siliceous sediment. Marine Biology, 46: 283-293, 1978.

Henry J.C. and Fisher S.G.. Spatial segregation of periphyton communities in a desert stream: causes and consequences for N cycling. Journal of The North American Benthological Society, 22 (4): 511-527, 2003.

He S. and Xu Y.J.. Three decadal inputs of nitrogen and phosphorus from four major coastal rivers to the summer hypoxic zone of the northern Gulf of Mexico. Water, Air, and Soil Pollution, 226: 311, 2015. DOI 10.1007/s11270-015-2580-6

Jäger C.G. and Borchardt D.. Longitudinal patterns and response lengths of algae in riverine ecosystems: A model analysis emphasizing benthic-pelagic interactions. Journal of Theoretical Biology, 442: 66-78, 2018.

Jäger C.G., Hagemann J., and Borchardt D.. Can nutrient pathways and biotic interactions control eutrophication in riverine ecosystems? Evidence from a model driven mesocosm experiment. Water Research, 115: 162-171, 2017.

Kuenen J.. Anammox bacteria: from discovery to application. Nature Reviews Microbiology, 6: 320-326, 2008. doi:10.1038/nrmicro1857

Kopáček J., Borovec J., Hejzlar J., Ulrich K., Norton S.A., and Amirbahman A.. Aluminum control of phosphorus sorption by lake sediments. Environmental Science & Technology, 39 (22): 8784-8789, 2005. DOI: 10.1021/es050916b

Kleeberg A., Hupfer M., and Gust G.. Phosphorus entrainment due to resuspension in a lowland river, Spree, NE Germany-A laboratory microcosm study. Water, Air, and Soil Pollution, 183(1-4): 129-142, 2007.

Kabenge M., Wang H., and Li F.. Urban eutrophication and its spurring conditions in the Murchison Bay of Lake Victoria. Environmental Science and Pollution Research, 23: 234-241, 2016. DOI 10.1007/s11356-015-5675-0

Lijklema L.. Nutrient dynamics in shallow lakes: effects of changes in loading and role of sediment-water interactions. Hydrobiologia, 275/276: 335-348, 1994.

570 Le Moal M., Cascuel-Odoux C., Menesguen A., Souchon Y., Etrillard C., Levain A., Moatar F., Pannard A., Souchu P.,
571 Lefebvre A., and Pinay G.. Eutrophication: A new wine in an old bottle. Science of the Total Environment, 651: 1-11, 2019.
572 Lyvén B., Hassellöv M., Turner D.R., Haraldsson C., and Andersson K. Competition between iron- and carbon-based colloidal
573 carries for trace metals in a freshwater assessed using flow field-flow fractionation coupled to ICPMS. Geochimica et
574 Cosmochimica Acta, 67(20): 3791-3802, 2003.
575 Li H., Song C.L., Cao X.Y., and Zhou Y.Y.. The phosphorus release pathways and their mechanisms driven by organic carbon
576 and nitrogen in sediments of eutrophic shallow lakes. Science of the Total Environment, 572: 280-288, 2016.
577 Lofts S., Tipping E., Hamilton-Taylor J.. The Chemical Speciation of Fe(III) in Freshwaters. Aquatic Geochemistry, 14(4):
578 337-358, 2008.
579 Lu H., Wang J., Li J., Shao H., and Wu Y.. Periphytic biofilm: A buffer for phosphorus precipitation and release between
580 sediments and water. Chemosphere, 144: 2058-2064, 2016.
581 Middelburg J.J.. Marine Carbon Biogeochemistry - A Primer for Earth System Scientists. Springer Briefs in Earth System
582 Sciences. Switzerland, 2019.
583 Mosley L. M., Hunter K. A., and Ducker W. A.. Forces between Colloid Particles in Natural Waters
584 Environmental Science & Technology, 37 (15): 3303-3308, 2003. DOI: 10.1021/es026216d
585 McGlathery K.J., Anderson I.C., and Tyler A.C.. Magnitude and variability of benthic and pelagic metabolism in a temperate
586 coastal lagoon. Marine Ecology Progress Series, 216: 1-15, 2001.
587 Middleburg J.J. and Nieuwenhuize J.. Uptake of dissolved inorganic nitrogen in turbid, tidal estuaries. Marine Ecology
588 Progress Series, 192: 79-88, 2000.
589 Miller M.P., Tesoriero A.J., Capel P.D., Pellerin B.A., Hyer K.E., and Burns D.A.. Quantifying watershed-scale groundwater
590 loading and instream fate of nitrate using high-frequency water quality data. Water Resources Research, 52: 330-347, 2016.
591 Mulder A., van de Graaf A.A., Robertson L.A., and Kuenen J.G.. Anaerobic ammonium oxidation discovered in a denitrifying
592 fluidized bed reactor. FEMS Microbiology Ecology, 1(16): 177-184, 1995.
593 Nyenje P.M., Foppen J.W., Uhlenbrook S., Kulabako R., and Muwanga A.. Eutrophication and nutrient release in urban areas
594 of sub-Saharan Africa-A review. Science of the Total Environment, 408: 447-455, 2010.
595 Painter H.A.. A review of literature on inorganic nitrogen metabolism in microorganisms. Water Research, 4: 393-450, 1970.
596 Pasterank A., Hillebrand H., and Flöder S.. Competition between benthic and pelagic microalgae for phosphorus and light-
597 long-term experiments using artificial substrates. Aquatic Sciences, 71: 238-249, 2009.
598 Putt A.E., MacIsaac E.A., Herunter H.E., Cooper A.B., and Selbie D.T.. Eutrophication forcings on a peri-urban lake
599 ecosystem: Context for integrated watershed to airshed management. PLoS ONE, 4(7): e0219241, 2019. https://doi.org/
600 10.1371/journal.pone.0219241
601 Paerl, H.W., Scott, J.T., McCarthy, M.J., Newell, S.E., Gardner, W.S., Havens, K.E., Hoffman, D.K., Wilhelm, S.W.,
602 Wurtsbaugh, W.A. It Takes Two to Tango: When and Where Dual Nutrient (N & P) Reductions Are Needed to Protect Lakes
603 and Downstream Ecosystems. Environmental Science and Technology, 50: 10805-10813, 2016.
604 https://doi.org/10.1021/acs.est.6b02575
605 Rozemeijer J.C. and Broers H.P.. The groundwater contribution to surface water contamination in a region with intensive
606 agricultural land use (Noord-Brabant, The Netherlands). Environmental Pollution. 148(3): 695-706, 2007.
607 Rozemeijer J.C., van der Velde Y., van Geer F.C., Bierkens M.F.P., and Broers H.P.. Direct measurements of the tile drain
608 and groundwater flow route contributions to surface water contamination: From field-scale concentration patterns in
609 groundwater to catchment-scale surface water quality. Environmental Pollution, 158: 3571-3579, 2010a.
610 Rozemeijer J.C., van der Velde Y., van Geer F.C., de Rooij G.H., Torfs P.J.J.F. and Broers H.P.. Improving load estimates for
611 NO3 and P in surface water by characterizing the concentration response to rainfall events. Environmental Science &
612 Technology. 44 (16): 6305-6312, 2010b.

https://doi.org/10.5194/hess-2020-34
Preprint. Discussion started: 26 February 2020

Rode M., Wade A.J., Cohen M.J., Hensley R.T., Michael J. Bowes, Kirchner J.W., Arhonditsis G.B., Jordan P., Kronvang B., Halliday S.J., Skeffington R., Rozemeijer J., Aubert A.H., Rinke K., and Jomaa S.. Sensors in the stream: the high-frequency wave of the present. Environmental Science & Technology, 50: 10297-10307, 2016.

Scheffer, M.. Ecology of shallow lakes, 1st edition. London: Chapman & Hall, 1998.

Spears B.M., Carvalho L.., Perkins R., Kirika A., and Paterson D.M.. Sediment phosphorus cycling in a large shallow lake: spatio-temporal variation in phosphorus pools and release. Hydrobiologia, 584: 37-48, 2007. https://doi.org/10.1007/s10750-007-0610-0

Smolders A. J. P., Lamers L. P. M., Lucassen E. C. H. E. T., Van Der Velde G. and Roelofs J. G. M.. Internal eutrophication: How it works and what to do about it—a review. Chemistry and Ecology, 22(2): 93-111, 2006. DOI: 10.1080/02757540600579730

Strayer D.L., Pace M.L., Caraco N.F., Cole J.J., and Findlay S.E.G.. Hydrology and grazing jointly control a large-river food web. Ecology, 89(1): 12-18, 2008.

Thamdrup B. and Dalsgaard T.. Production of N2 through anaerobic ammonium oxidation coupled to nitrate reduction in marine sediments. Applied and Environmental Microbiology, 68(3): 1312-1318, 2002.

Toor G.S., Occhipinti M.L., Yang Y.Y., Majcherek T., Haver D., and Oki L.. Managing urban runoff in residential neighbourhoods: Nitrogen and phosphorus in lawn irrigation driven runoff. PLoS ONE, 12(6): e0179151, 2017. https://doi.org/10.1371/journal.pone.0179151

Van der Grift, B., Broers, H.P., Berendrecht, W., Rozemeijer, J., Osté, L., and Griffioen, J.. High-frequency monitoring reveals nutrient sources and transport processes in an agriculture-dominated lowland water system. Hydrology and Earth System Sciences, 20(5): 1851-1868, 2016.

Van Geer F.C., Kronvang B., and Broers H.P.. High-resolution monitoring of nutrients in groundwater and surface waters: process understanding, quantification of loads and concentrations, and management applications. Hydrology and Earth System Sciences, 20: 3619-3629, 2016.

Van der Grift B., Osté L., Schot P., Kratz A., van Popta E., Wassen M., and Griffioen J.. Forms of phosphorus in suspended particulate matter in agriculture-dominated lowland catchments: Iron as phosphorus carrier. Science of The Total Environment, 631-632: 115-129, 2018.

Van der Grift B., Rozemeijer J.C., Griffioen J., and van der Velde Y.. Iron oxidation kinetics and phosphate immobilization along the flow-path from groundwater into surface water. Hydroloy Earth System Science, 18: 4687-4702, 2014.

Wilczak A., Jacangelo, J.G., Marcinko J.P., Odell L.H., Kirmeyer G.J.. Occurrence of nitrification in chloraminated distribution systems. Journal AWWA, 88(7):74-85, 1996.

Wang T., Liu G., Gao L., Zhu L., Fu Q., and Li D.. Biological and Nutrient Responses to a Typhoon in the Yangtze Estuary and the Adjacent Sea. Journal of Coastal Research, 32(2): 323-332.

Walsh C.J., Roy J.W., Feminella J.W., Cottingham P.D., Groffman P.M., and Morgan II R.P.. The urban stream syndrome: current knowledge and the search for a cure. Journal of The North American Benthological Society, 24(3): 706-732, 2005.

Wriedt, G., Spindler J., Neef T., Meißner R., and Rode M.. Groundwater dynamics and channel activity as major controls of in-stream nitrate concentrations in a lowland catchment system? Journal of Hydrology, 343: 154–168, 2007.

Yu L., Rozemeijer J.C., van Breukelen B.M., Ouboter M., van der Vlugt C., and Broers H.P.. Groundwater impacts on surface water quality and nutrient loads in lowland polder catchments: monitoring the greater Amsterdam area. Hydrology and Earth System Sciences, 22:487-508, 2018.

Yu L., Rozemeijer J.C., van der Velde Y., van Breukelen B.M., Ouboter M., and Broers H.P.. Urban hydrogeology: Transport routes and mixing of water and solutes in a groundwater influenced urban lowland catchment. Science of the Total Environment, 678: 288-300, 2019.

https://doi.org/10.5194/hess-2020-34
Preprint. Discussion started: 26 February 2020

655 Yang Y.Y. and Toor G.S.. Stormwater runoff driven phosphorus transport in an urban residential catchment: Implications for
656 protecting water quality in urban watersheds. Scientific Reports, 8, 11681, 2018. doi:10.1038/s41598-018-29857-x
657 Zhu W.X., Dillard N.D., and Grimm N.B.. Urban nitrogen biogeochemistry: status and processes in green retention basins.
658 Biogeochemistry, 71: 177-196, 2004.
659 Zhang X. and Mei X.. Effects of benthic algae on release of soluble reactive phosphorus from sediments: a radioisotope tracing
660 study. Water Science and Engineering, 8(2): 127-131, 2015.
661 Zhang W., Jin X., Meng X., Tang W., and Shan B.. Phosphorus transformations at the sediment-water interface in shallow
662 freshwater ecosystems caused by decomposition of plant debris. Chemosphere, 201: 328-334, 2018.
663 Zhou L., Wang S., Zou Y., Xia C., and Zhu G.. Species, abundance and function of ammonia-oxidizing Archaea in inland
664 waters across China. Scientific Reports, 5: 15969, 2015. DOI: 10.1038/srep15969
665

https://doi.org/10.5194/hess-2020-34
Preprint. Discussion started: 26 February 2020

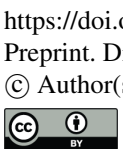

Hydrology and Earth System Sciences
Discussions
Open Access
EGU

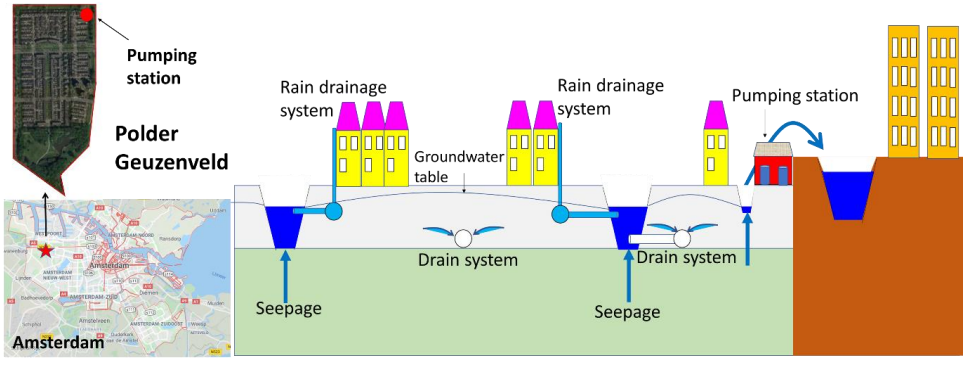

Figure 1 Location of polder Geuzenveld (source: © Google Maps) and its landscape cross section and rain water and groundwater drainage system.

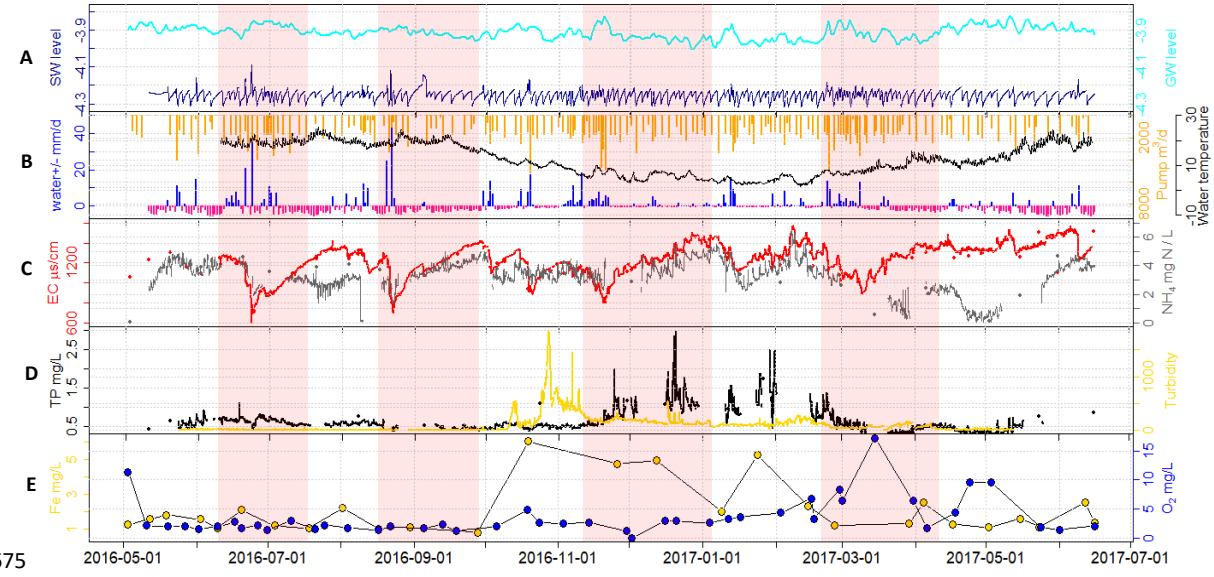

Figure 2 Time series of (A) surface water level (SW level) and groundwater level (m NAP), (B) daily water surplus (+) (blue) and deficiency (-) (pink) and daily pumping volume (Pump m^3 d-1), (C) hourly time series data of EC (µS/cm) and NH_4-N (mg N L^{-1}), and (D) hourly time series of TP, turbidity, (E) discrete samples of Fe (total iron in water column) and O_2 concentrations (mg L^{-1}). The red, grey and black dots in (C) and (D) are the corresponding discrete sampling data, which are plotted to show their close match to the continuous time series data, as well as to fill in the gaps. Red blocks are selected rain events for further analysis in section 3.3.

https://doi.org/10.5194/hess-2020-34
Preprint. Discussion started: 26 February 2020

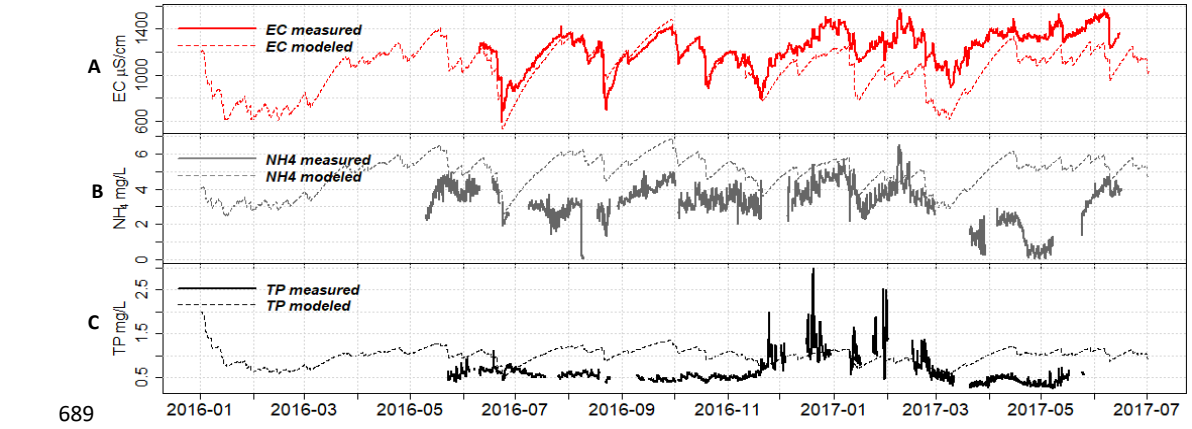

Figure 3 Plots of fixed-end-member mixing model predicted (A) EC, (B) NH_4 and (C) TP with their measured time series data.

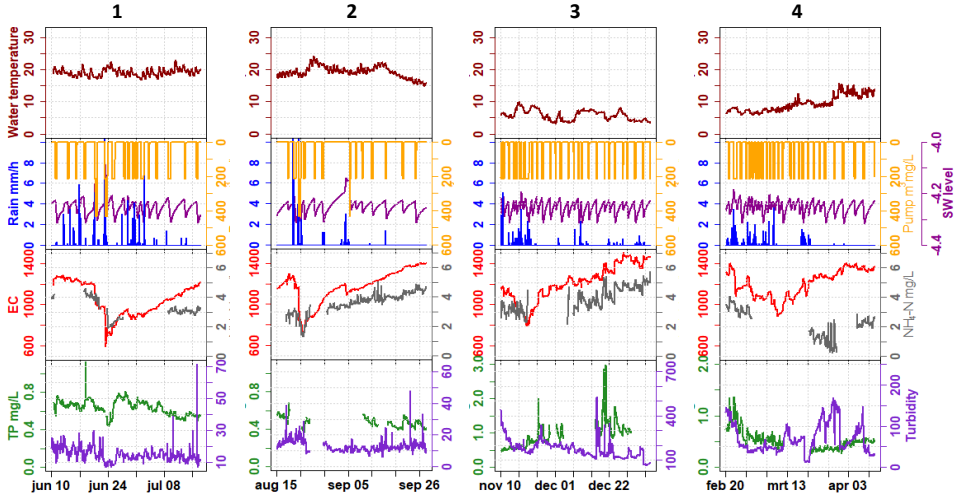

Figure 4 Selected events showing dilution and peaks of water quality parameters, with hourly precipitation (mm/h) and hourly pumping activity (m^3/h). Note that between events different scales of TP and turbidity were used to reveal the dynamics.

https://doi.org/10.5194/hess-2020-34
Preprint. Discussion started: 26 February 2020

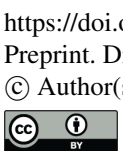

Hydrology and Earth System Sciences
Discussions

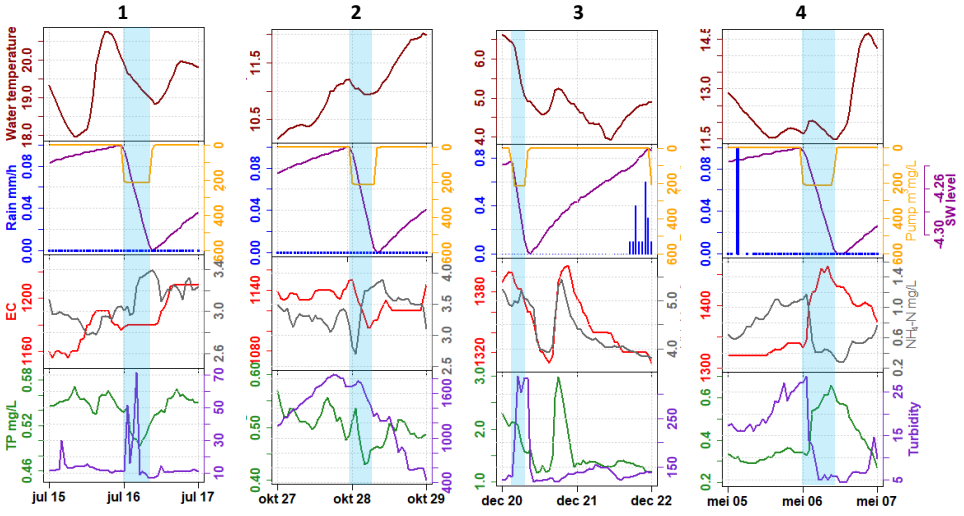

Figure 5 Pumping and day and night patterns of water quality, blue blocks represent pumping duration

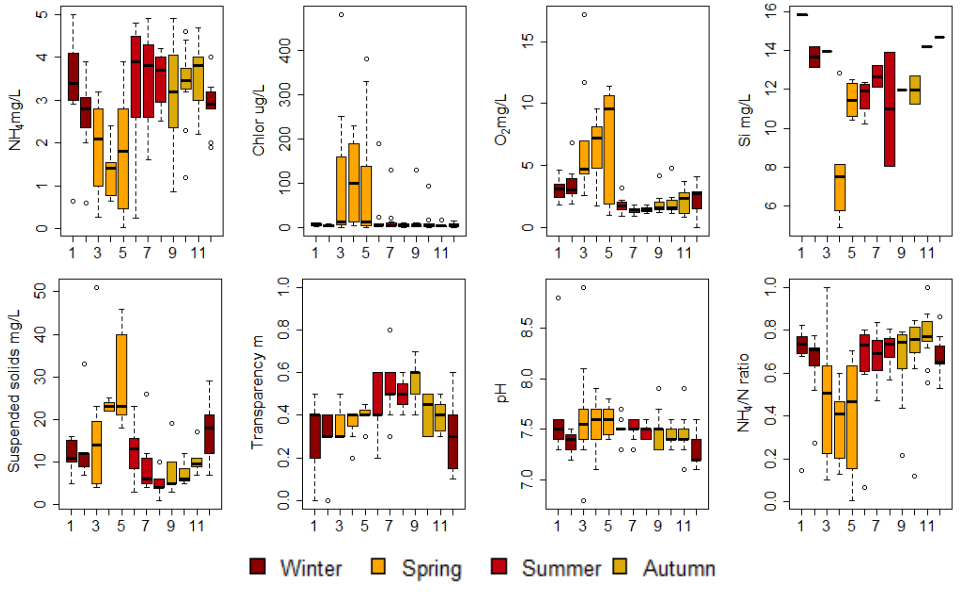

Figure 6 Monthly measurement of NH_4, chlorophyll-a (Chlor), O_2, suspended solids and water transparency, pH and NH_4/TN (NH_4/N) mass ratio in Geuzenveld from 2007-2018. X axis is month.

https://doi.org/10.5194/hess-2020-34
Preprint. Discussion started: 26 February 2020

Hydrology and Earth System Sciences
Discussions

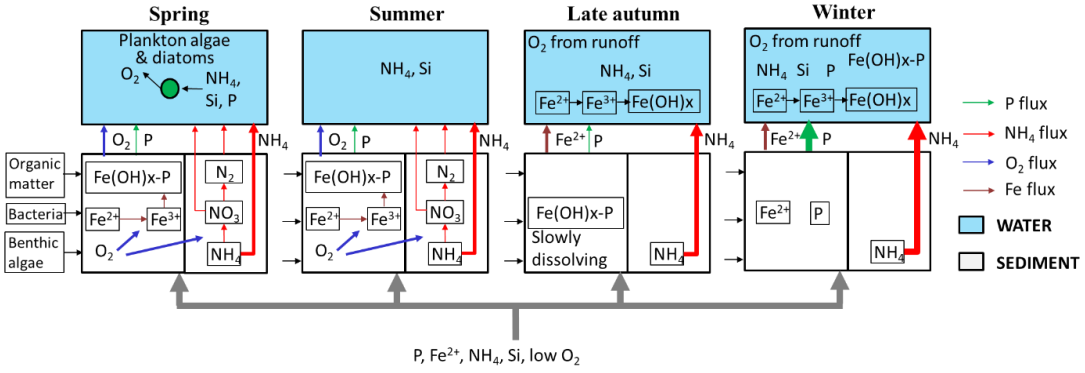

Figure 7 Schematic representation of N and P dynamics in spring, summer, later autumn and winter. The thickness of the flow lines represents the concentration magnitudes, the thicker the line, the higher the concentrations.

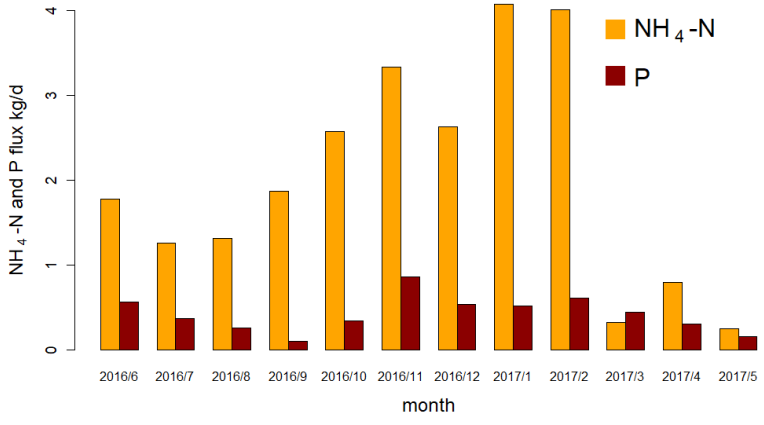

Figure 8 Average daily NH_4-N and P flux (kg per day) in each month in the discharge (calculated from the continuous measurements) of polder Geuzenveld from June 2016 to May 2017.

Table 1 Pumping scheme of polder Geuzenveld

Time	Settings	Pump 1	Pump 2
05:00:00-19:00:00	Start point (m NAP)	-4.20	-4.16
	End point (m NAP)	-4.26	-4.24
19:00:00-05:00:00	Start point (m NAP)	-4.23	-4.18
	End point (m NAP)	-4.31	-4.29

https://doi.org/10.5194/hess-2020-34
Preprint. Discussion started: 26 February 2020

Hydrology and Earth System Sciences
Discussions

***Code/data availability*:** The code scripts and datasets related to this paper are available on request to Liang Yu, contact is xiaobaidrawing@gmail.com.

Author contribution: Maarten Ouboter, Joachim Rozemeijer, and Hans Peter Broers funded this research. Hans Peter Broers and Joachim Rozemeijer designed the field work. Liang Yu carried out the field work and the data collection, analysis, visualization, discussion, and the writing of the manuscript, under the supervision of Hans Peter Broers and Joachim Rozemeijer before 2019, Ype van der Velde as the main supervisor since 2019. All the authors participated the discussion of the data analysis results, and helped prepare the manuscript.

Competing interests: The authors declare that there is no conflict of interest.